Open

Oncogene (2013) **32,** 5101–5110

www.nature.com/onc

ORIGINAL ARTICLE

Metabolic intervention on lipid synthesis converging pathways abrogates prostate cancer growth

V Fritz[1,2,3], Z Benfodda[4,5,13], C Henriquet[6,13], S Hure[1,2,3], J-P Cristol[7,8], F Michel[7,8], M-A Carbonneau[9], F Casas[10] and L Fajas[1,2,3,11,12]

One of the most conserved features of all cancers is a profound reprogramming of cellular metabolism, favoring biosynthetic processes and limiting catalytic processes. With the acquired knowledge of some of these important changes, we have designed a combination therapy in order to force cancer cells to use a particular metabolic pathway that ultimately results in the accumulation of toxic products. This innovative approach consists of blocking lipid synthesis, at the same time that we force the cell, through the inhibition of AMP-activated kinase, to accumulate toxic intermediates, such as malonyl-coenzyme A (malonyl-CoA) or nicotinamide adenine dinucleotide phosphate. This results in excess of oxidative stress and cancer cell death. Our new therapeutic strategy, based on the manipulation of metabolic pathways, will certainly set up the basis for new upcoming studies defining a new paradigm of cancer treatment.

Oncogene (2013) **32,** 5101–5110; doi:10.1038/onc.2012.523; published online 3 December 2012

Keywords: lipids; cancer; FAS; metabolism; prostate

INTRODUCTION

Metabolic changes are key early events during cellular transformation. Increased glycolytic ratio, high lactate production and augmented *de novo* lipid synthesis have been well documented in most types of cancer. Most adult normal cells and tissues, even those with high cellular turnover, preferentially use circulating fatty acids (FAs) for the synthesis of new structural and signaling lipids. In contrast, it is now well documented that various tumors and their precursor lesions, including prostate cancer (PC), undergo exacerbated endogenous FA biosynthesis, irrespective of the levels of extracellular lipids. These specific metabolic features of cancer cells have been used to define new metabolic targets for cancer therapy. Abrogation of lipid synthesis through inhibition of lipogenic enzymes, such as the FA synthase (FASN),[1,2] ATP-citrate lyase, acetyl-coenzyme A (acetyl-CoA) carboxylase (ACC)[3] or stearoyl-CoA desaturase,[4] results in decreased proliferation and increased apoptosis of cancer cells (reviewed in Fritz and Fajas[5]). The cytotoxic effects of these experimental therapies are probably secondary to the inhibition of the synthesis of specific lipids, such as phosphatidyl inositols, or phosphatidic acids, which are essential for cancer cell growth. In addition, accumulation of toxic intermediates could also account for the observed increase in apoptosis of cancer cells. Indeed, it has been suggested that the cytotoxicity induced by FASN inhibition may be the result of malonyl-CoA accumulation, which is a toxic intermediate.[6,7] In addition, inhibition of lipid synthesis has a strong impact on general metabolism. For instance, *de novo* lipogenesis requires nicotinamide adenine dinucleotide phosphate (NADPH), which is generated by the pentose phosphate pathway, or by malate dehydrogenases and malic enzyme, as a cofactor for the synthesis of palmitate by FASN. Inhibition of lipid synthesis will therefore result in the accumulation of NADPH, which can be transformed in reactive oxygen species (ROS) in cancer cells.

In this study, we used a new therapeutic approach based on the previous observation that malonyl-CoA accumulation results in apoptosis of cancer cells. We hypothesized that inhibition of malonyl-CoA utilization, as a substrate for palmitate synthesis, through blocking of FASN activity, together with the induction of the activity of ACC, which produces malonyl-CoA from acetyl-CoA, would result in further accumulation of malonate and therefore increased apoptosis of PC cells. Hyperactivity of ACC was achieved through inactivating AMP-activated kinase (AMPK), which phosphorylates and inhibits ACC activity.

Here we show that this experimental approach resulted not only in the accumulation of malonyl-CoA but also in the activation of NADPH-producing ME, which leads to a cytotoxic generation of NADPH oxidase (NOX)-dependent oxidative stress, ultimately resulting in the abrogation of tumor growth in a mice model of PC.

RESULTS

Combined AMPK and FASN inhibition induces malonyl-CoA accumulation in PC cells

Malonyl-CoA accumulation has been previously shown to be toxic for cancer cells.[6] During *de novo* lipid synthesis, malonyl-CoA is produced from acetyl-CoA precursor by ACC and then converted

[1]IGMM, CNRS, Institut de Génétique Moléculaire de Montpellier, Montpellier, France; [2]CNRS, UMR5535, Montpellier, France; [3]Université de Montpellier 2, Montpellier, France; [4]IBMM, Institut des Biomolécules Max Mousseron CNRS UMR5247 CC 1706, Laboratoire des Acides Aminés, Peptides et Protéines – Université de Montpellier 2, Montpellier, France; [5]Laboratoire de Chimie Bioorganique, Université de Nîmes, Nimes, France; [6]IRCM, Institut de Recherche en Cancérologie de Montpellier, Montpellier, France; [7]Laboratoire de Biochimie, Centre Hospitalier Universitaire Lapeyronie, Montpellier, France; [8]UMR 204 Prévention des Malnutritions et des Pathologies Associées, Institut Universitaire de Recherche Clinique, Montpellier, France; [9]UMR 204 NUTRIPASS, Institut Universitaire des Recherches Cliniques, Montpellier, France; [10]INRA UMR 0866, Montpellier, France; [11]Centre Hospitalier Régional Universitaire de Montpellier, Montpellier, France and [12]Department of Physiology, Université de Lausanne, Lausanne, Switzerland. Correspondence: Professor L Fajas, IGMM, CNRS, Institut de Génétique Moléculaire de Montpellier, 1919 route de mende, Montpellier 34293, France.
E-mail: lluis.fajas@unil.ch
[13]Co second authors.
Received 25 May 2012; revised 21 September 2012; accepted 28 September 2012; published online 3 December 2012

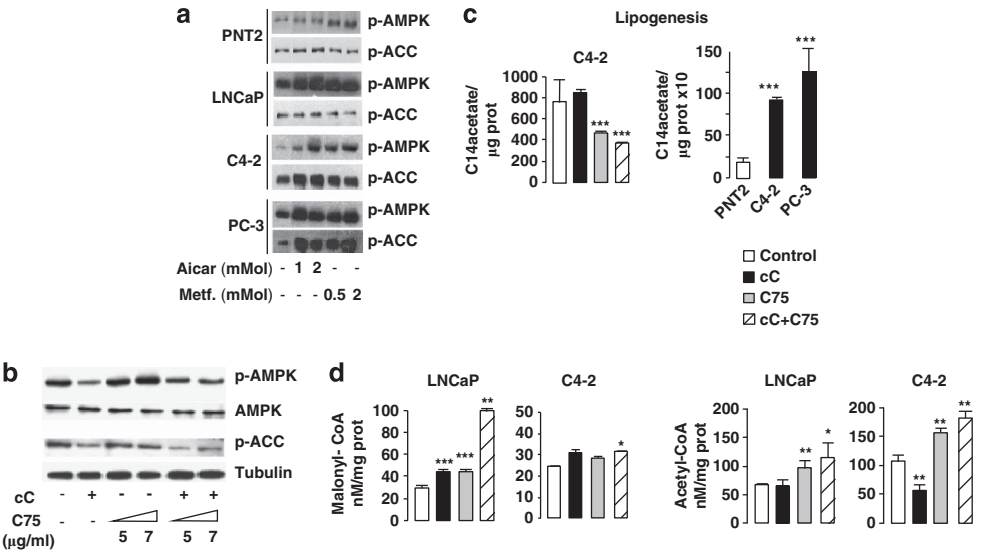

Figure 1. Combined AMPK and FASN inhibition induces malonyl-CoA accumulation in PC cells. The AMPK and FASN inhibitors' concentration used in all *in vitro* experiments were as follows: cC 1 μg/ml, araA 0.5 mM and C75 7 μg/ml, unless otherwise indicated. (**a**) Immunoblot analysis of phospho (p)-AMPK and p-ACC in PNT2, LNCaP, C4-2 and PC-3 cell lines at 24 h following treatment with increasing concentration of AMPK activators AICAR or metformin (Metf.). (**b**) Immunoblot analysis of p-AMPK, total AMPK, p-ACC and tubulin in the LNCaP cell line at 24 h following treatment with either 1 μg/ml cC alone, 5–7 μg/ml C75 alone or with cC combined to increasing C75 concentrations. (**c**) Lipid synthesis through [^{14}C]palmitate incorporation into TAG was measured in C4-2 cells at 24 h following treatment with either cC, C75 or cC + C75 (left panel). Basal lipid synthesis levels were quantified in normal prostate PNT2 cells compared with C4-2 and PC-3 PC cells. (**d**) Cellular contents in malonyl-CoA and acetyl-CoA were measured in PNT2, LNCaP or C4-2 cells at 24 h following treatment with either cC, C75 or with combined cC + C75 treatment.

to palmitic acid by the FASN enzymatic complex. ACC activity is inhibited by AMPK phosphorylation. Inhibition of AMPK should therefore result in increased ACC activity and increased malonyl-CoA synthesis. Furthermore, concomitant inhibition of FASN should result in decreased malonyl-CoA utilization, and overall malonyl-CoA accumulation. Before testing this hypothesis, we first analyzed the status of AMPK activity in non-tumoral PNT2 and tumoral LNCaP, C4-2 and PC-3 human prostate cell lines, under control culture conditions or in the presence of increasing concentrations of the AMPK activators AICAR or metformin. AMPK activity was evaluated by assessing the phosphorylation status of the AMPK activation loop (Thr172) and its direct substrate ACC (Ser79). Immunoblot analysis demonstrated basal AMPK activity in non-tumor and tumor cell lines, probably secondary to cell culture stress conditions (Figure 1a). Treatment of the cells with AICAR and metformin revealed, however, robust increases of phospho-AMPK and phospho-ACC levels, suggesting increased AMPK activity. Interestingly, increased AMPK activity, as measured by changes in ACC phosphorylation, was significantly higher in the more aggressive PC cell lines C4-2 and PC-3, compared with normal prostate cell line PNT2 or hormone-sensitive LNCaP cells (Figure 1a).

We next tested the hypothesis that concomitant inhibition of FASN and AMPK would result in malonyl-CoA accumulation and overall decreased *de novo* lipid synthesis in these cells. Treatment of LNCaP PC cells with compound C (cC) significantly decreased AMPK activation, as demonstrated by decreased phosphorylation (Figure 1b). Consistently, cC treatment efficiently inhibited ACC phosphorylation. Total AMPK levels were not changed in response to cC. Treatment of PC cells with C75 showed no impact on AMPK and ACC phosphorylation, whereas treatment with cC combined with C75 decreased AMPK and ACC phosphorylation to a similar extent compared with cC alone (Figure 1b). Consistent with the inhibition of FAS activity, treatment of the cells with C75 in the absence or presence of cC resulted, as expected in inhibition of *de novo* lipid synthesis, in PC cells (Figure 1c, left panel). [^{14}C]acetate was used by the cells to synthesize FAs, which are subsequently incorporated into TAGs. All cancer cell lines tested showed a decrease of ^{14}C incorporation in TAGs (Figure 1c). Most interesting was the observation that *de novo* lipid synthesis was almost not detectable and strongly decreased in the non-cancerous prostate cell line PNT2 (Figure 1c, right panel). This suggested that the toxic effects of the treatment should not be observed in normal cells, compared with PC cells, because non-tumor prostate cells do not have active lipid synthesis. This will be demonstrated in the following figures.

Interestingly, combined C + C75 treatment induced significant increase of both malonyl-CoA and acetyl-CoA levels in PC LNCaP cells (Figure 1d). The observation that in C4-2 cells individual treatments resulted only in mild increases in malonyl-CoA accumulation is intriguing, although a significant increase in malonyl-CoA levels was observed in cells co-treated with cC and C75 (Figure 1d). In contrast, a robust accumulation of acetyl-CoA was observed when C4-2 cells were treated with either C75 or the combination treatment. This suggested that unexpected mechanisms activated the conversion of malonyl into acetyl-CoA in response to FASN inhibition in these cells. Despite this, concomitant inhibition of FASN and AMPK activities results in the accumulation of malonyl-CoA, which is a toxic metabolite for the cell.

Combination treatments of AMPK and FASN inhibition abrogate PC cell growth and viability *in vitro*

Combination treatments were now tested for the effects on proliferation and cancer cell growth and viability. Inhibition of AMPK activity by cC treatment induced a significant decrease in cell proliferation in LNCaP (38%), C4-2 (33%) and PC-3 (32%) PC cells (Figure 2a). Similarly, inhibition of FASN induced a block in the proliferation of these cells, whereas the combined treatment with cC and C75 resulted in a further inhibition of cell proliferation, reaching 78%, 84% and 85% in LNCaP, C4-2 and PC-3 cells,

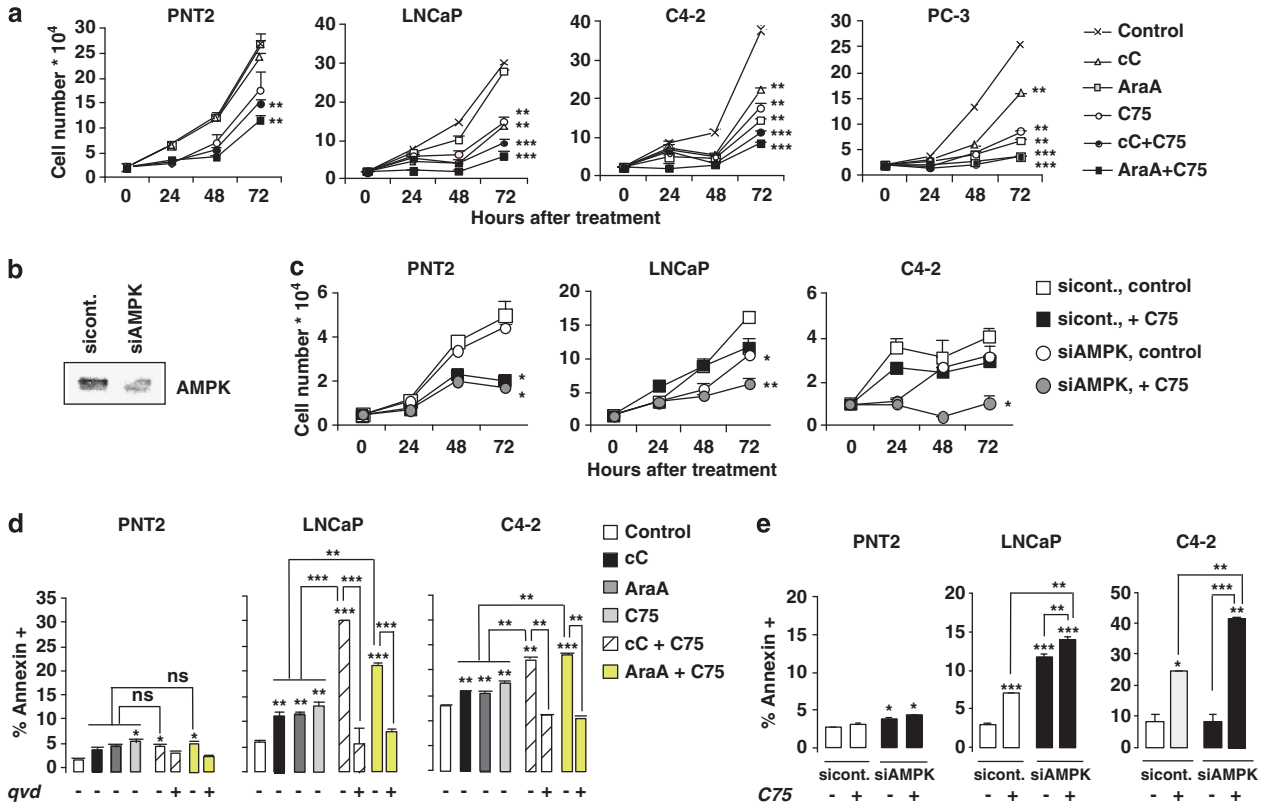

Figure 2. Combined AMPK and FASN inhibition blocks PC cells' proliferation *in vitro* and induces caspase-dependent apoptosis. (**a**) Effects of cC and C75 inhibitors on LNCaP and C4-2 cell proliferation was assessed by cell counting at the indicated times. (**b**–**e**) Genetic inhibition of AMPK in PNT2, LNCaP and C4-2 cells was performed by nucleofaction with siRNA against hAMPKα1/2. Reduced AMPKα1/2 expression is shown by AMPKα1/2 immunoblotting (**b**) in LNCaP cells 24 h after transfection with control or siRNA against hAMPKα1/2. (**c**) Proliferation of sicont- or siAMPKα1/2—PNT2, LNCaP or C4-2 cells was measured by cell counting following treatment with control or C75-supplemented media at the indicated times. (**d**) Effect on cell viability was analyzed by FACS by measuring the percentage of annexin V-FITC + cells at 16 h following treatment with control or C75-supplemented media at the indicated times. Rescue from apoptosis induction was analyzed following pre-treatment of cells with 20 μM qVD-oph caspase inhibitor. (**e**) Effect on cell viability was analyzed by FACS by measuring the percentage of annexin V-FITC + cells at 16 h after indicated siRNA treatments.

respectively, at 72 h. The specificity of the measure effect was confirmed by using another AMPK inhibitor, adenine 9-β-D-arabinofuranoside (AraA). Indeed, we showed that combined AraA + C75 treatment resulted in 80%, 77% and 84% in LNCaP, C4-2 and PC-3 cells, respectively, at 72 h (Figure 2a). In contrast, PNT2 cell proliferation was much less sensitive to the inhibition of AMPK activity by either cC or AraA. PNT2 cell proliferation was also decreased, but to a less extent than tumoral PC cells, at 72 h following cC + C75 treatment or AraA + C75 treatment (Figure 2a). Similar to that observed using AMPK inhibitors, genetic AMPKα1/2 inhibition using small interfering RNA (siRNA) technology, which reduced AMPKα1/2 protein expression (Figure 2b), resulted in 35% and 21% decrease of LNCaP and C4-2 tumor cell proliferation, respectively, but in only 10% decrease of non-tumoral PNT2 cell proliferation (Figure 2c). Upon addition of C75, proliferation of AMPKα1/2 knockdown LNCaP or C4-2 cells was markedly decreased by 62 and 75%, although proliferation of sicont.-LNCaP or C4-2 cells was decreased by 27% and 27%, respectively, as compared with control culture media. In contrast, upon addition of FASN inhibitor C75, proliferation of sicont- and siAMPKα1/2-PNT2 cells was reduced by 60% and 65%, respectively, at 72 h, indicating that AMPK does not have a crucial role in proliferation in non-tumoral PC cells, as compared with that observed in PC cells. This indicated that the effects of cC are mediated by AMPK.

Malonyl-CoA accumulation has been previously shown to induce apoptosis in cancer cells. The combined treatment using AMPK and FASN inhibitors is efficient in malonyl-CoA accumulation, which correlated with decreased viability of the cells. We therefore tested the effects on apoptosis of this treatment. The combination of cC and C75 inhibitors induced a significant 4.7- and 2-fold increase in the percentage of LNCaP and C4-2 cells positive for annexin V-fluorescein isothiocyanate (FITC), respectively, as compared with control, reflecting externalization of phosphatidylserine during early apoptosis (Figure 2d). Similarly, combination treatment of AraA and C75 induced a significant 3- and 2.2-fold increase in the percentage of LNCaP and C4-2 cells positive for annexin V-FITC. Moreover, the caspase inhibitor qVD-oph efficiently abrogated the effects of cC + C75 or AraA + C75 co-treatment on apoptosis (Figure 2d). In sharp contrast, only 5% of PNT2 cells were stained positive for annexin V-FITC following treatment with either C75 alone or with cC + C75 or AraA + C75 co-treatments, indicating that combined AMPK and FASN inhibition does not affect non-tumoral PNT2 cell viability. Moreover, cleaved caspase-3 immunostaining indicated the activation of caspase-dependent apoptosis in PC but not in PNT2 cells following AMPK and FASN inhibition by treatment with either cC + C75 or AraA + C75 (Supplementary Figure 1). Furthermore, cytochrome c immunostaining in C4-2 cells following cC + C75 or AraA + C75 treatment was diffuse and funter indicative of apoptotic induction, although it was intense and punctate in PNT2 cells, indicating that it has not been released from the mitochondria (Supplementary Figure 1).

Similar to that observed using AMPK inhibitors, the percentage of apoptotic annexin V-FITC + cells was significantly induced by

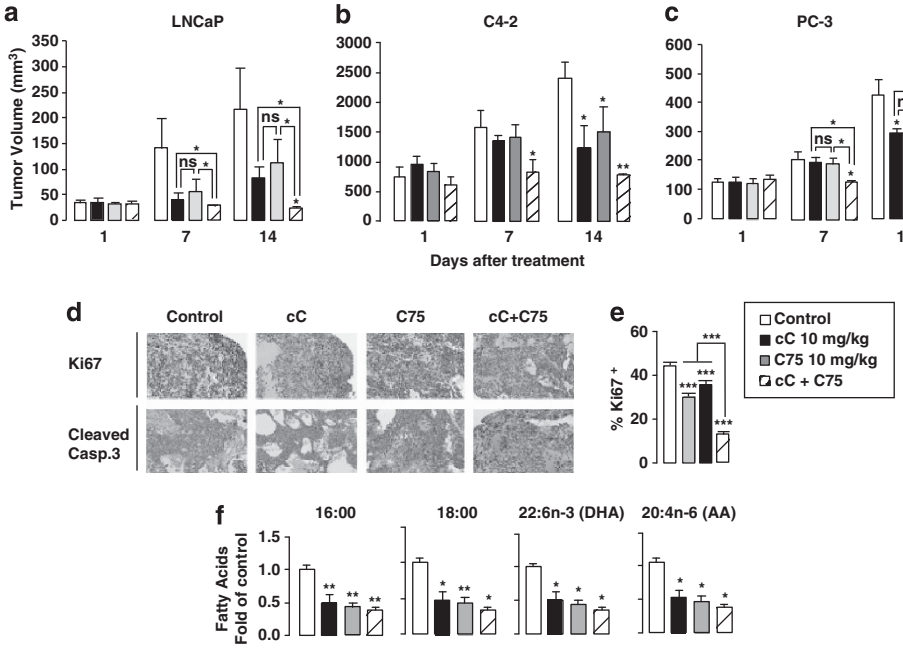

Figure 3. Combined AMPK and FASN inhibition reduces tumor growth in mice. (**a–c**) Tumor volume progression of subcutaneously implanted LNCaP (**a**), C4-2 (**b**) and PC-3 (**c**) cells in nude athymic mice was measured weekly following intraperitoneal injection with 10 mg/kg of either cC alone, C75 alone or both cC and C75 for 5 days a week. Values are expressed as the mean tumor volume (mm^3) ± s.e.m. ($n = 5$ for each group) from day 1 to day 14. (**d**) Ki67 and cleaved caspase-3 immunostaining of C4-2 tumor sections. (**e**) Quantification of cycling Ki67 + cells on C4-2 tumor sections. Six fields per section were analyzed for Ki67 immunostaining indicative of cell proliferation. Sections of tumors of all mice were analyzed. At least 300 cells were counted per tumor. (**f**) The lipidic composition was analyzed in total lipids extracted from C4-2 tumor tissues. Values are expressed as fold of control (mean ± s.e.m.).

3.9-fold in siAMPKα1/2 as compared with sicont-LNCaP cells, and it was further increased to 4.7- and 6-fold in siAMPKα1/2 LNCaP and siAMPKα1/2 C4-2 cells, respectively, upon addition of C75. In sharp contrast, only 1.4- and 1.5-fold increases of annexin V-FITC staining were induced in sicont.- and siAMPKα1/2-PNT2 cells treated with C75 as compared with the control media.

Combinations of AMPK and FASN inhibition abrogate PC cell growth in a mouse model of PC

Inhibition of cancer cell growth was further proved by *in vivo* experiments using a mouse model of PC. LNCaP, C4-2 and PC-3 cells were injected subcutaneously in male athymic nude mice. Treatment of each individual mouse started when tumor nodules were measurable. We observed that treatment of mice with 10 mg/kg of either cC alone, C75 alone or a combination of cC and C75 significantly inhibited both androgen-dependent LNCaP (Figure 3a) and androgen-insensitive C4-2 (Figure 3b) and PC-3 (Figure 3c) tumor volume and tumor growth rate, as compared with control mice that received vehicle only. Early efficiency of cC + C75 combined treatment was evidenced in LNCaP, C4-2 and PC-3 tumor xenografts by a 80%, 47% and 37% decrease, respectively, in mean tumor volume as soon as day 7, reaching 89%, 67% and 65% at day 14, as compared with the control group. In contrast, cC individual treatment induced significant tumor volume decrease only by day 14 in LNCaP, C4-2 and PC-3 xenografts, whereas C75 individual treatment induced significant tumor volume decrease (60%) by day 7 only in LNCaP tumor xenografts (Figures 3a–c). On day 7 of treatment, we observed that C4-2 tumor volume was increased more than twofold in 63% of vehicle-treated mice and more than threefold in 50% of them, whereas this was observed only in 20% of cC + C75-treated mice (Figure 3b). These results suggested that the combination of AMPK and FASN inhibition has cytotoxic effects that result in the abrogation of tumor growth *in vivo*.

Immunostaining of tumors from C4-2 xenografts for the cell cycle entry-associated marker Ki67 further supported the efficiency of combined cC + C75 treatment to inhibit tumor cell proliferation with an average 73% decrease of Ki67 + cells in tumors, compared with tumors from control animals (Figure 3e). Importantly, the decrease of Ki67 + cells was associated with an increase of cleaved caspase-3 + cells in C4-2 tumors from animals treated with cC + C75, as compared with animals that received control or single treatments (Figure 3d). This indicates that combined AMPK and C75 inhibition may induce apoptosis in PC tumors *in vivo*. We next investigated whether the reduction of tumor growth following combined AMPK and FASN inhibition was associated with changes in FA composition *in vivo*. Analysis of total lipids extracted from tumor tissues revealed an overall decrease in lipid content in mice receiving cC + C75 treatment, as compared with control mice, and more specifically a significant decrease in palmitate (16:0) (24%), stearate (18:0) (34%), arachidonic acid (20:4*n*-6) (30%) and DHA (22:6*n*-3) (29%) FAs' contents (Figure 3f). This suggested that the observed effects of cC + C75 treatment on tumor growth are mediated, at least in part, by inhibition of lipid synthesis.

Importantly, no significant weight loss or other toxicity was observed in mice following daily intraperitoneal injections of cC and or C75 (Supplementary Figure 2). Histological examination confirmed the absence of toxicity in the liver, and no difference of tissue integrity between control and treated animals (Supplementary Figure 2). Moreover, hematocrit analysis revealed normal erythropoiesis in treated vs control animals (Supplementary Figure 2).

Increased ME1 activity mediates the effect of AMPK and FAS inhibition on PC cell proliferation

We next asked how AMPK inhibition could decrease tumor growth and induce apoptosis in the context of blocked lipid synthesis.

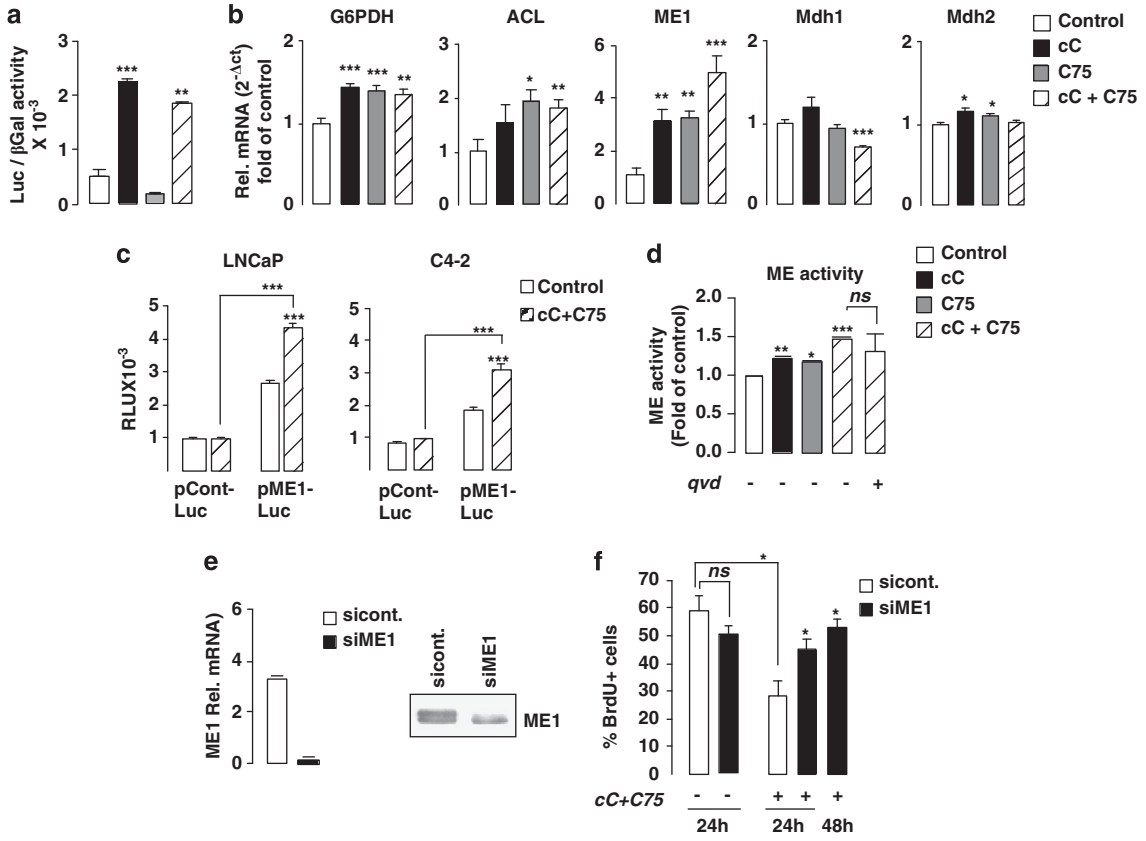

Figure 4. Combined AMPK and FASN inhibition in PC cells is associated with an increased ME activity. (**a**) Induction of the SREBP-1 transcriptional activity following cC + C75 co-treatment was assessed by measuring firefly Luc activity in LNCaP cells overexpressing SREBP-1 and FAS-Luc promoters, as compared with control. Values are expressed as relative luciferase unit (RLU) normalized relative to the β-galactosidase activity. (**b**) Variations in mRNA expression levels of SREBP-1 target genes *G6PDH*, *ATP-citrate lyase*, *ME1* and malate dehydogenases (*Mdh*)-1 and -2 were analyzed by RT-qPCR in LNCaP cells at 24 h following indicated treatments. (**c**) Induction of the ME1 transcriptional activity following cC + C75 co-treatment was assessed by measuring Renilla luciferase (Luc) activity in LNCaP and C4-2 cells overexpressing ME1-Luc promoter, as compared with control. Values are expressed as relative luciferase unit (RLU) normalized relative to the β-galactosidase activity. (**d**) Induction of ME enzymatic activity in whole LNCaP cells was analyzed by spectrophotometry in the presence of NADPH substrate at 24 h following indicated treatments. (**e**) Rescue from the antiproliferative effect of cC + C75 treatment in LNCaP cells was conducted by genetic inhibition of ME1. ME mRNA and protein expression is indicated. (**f**) Quantification of the percentage of BrdU-incorporating cells transfected with siRNA against ME1, as compared with control.

AMPK is known to inhibit SREBP-1 activity, which regulates the expression of genes implicated in lipid synthesis, and also genes implicated in the generation of ROS, such as the glucose-6-phosphate dehydrogenase (G6PDH). Indeed, SREBP-1 transcriptional activity was induced 4.4- and 3.6-fold at 12 h following cC and cC + C75 treatment, respectively (Figure 4a), in LNCaP cells, consistent with an inhibitory effect of AMPK on SREBP activity. Moreover, mRNA expression of the SREBP-1 target genes *G6PDH* and *ATP-citrate lyase* was induced 1.4- and 1.5-fold, respectively, in LNCaP cells after 24 h of cC treatment (Figure 4b). No further induction in the expression of these genes was observed when cells were co-treated with cC + C75 or when the expression of malate dehydogenases 1 and 2 was analyzed. In contrast, ME1 mRNA level was further increased up to 4.4-fold when cells were treated with the cC + C75 combination treatment, compared with the 2.8-fold increase observed with each individual treatment (Figure 4b). The increase in ME1 mRNA concentration correlated with the induction of the ME1 promoter (Figure 4c) and with significant changes in ME enzymatic activity (Figure 4d) upon treatment. Importantly, the pre-treatment of cells with the caspase inhibitor qVD-oph had no effect on measured ME activity following the different treatments (Figure 4d). Similar results were obtained in C4-2 and PC-3 cells (data not shown). These results suggested that ME1 activity was mediating, at least in part, the proapoptotic effects of the treatment. To test this hypothesis, ME1 was silenced in LNCaP cells using specific siRNA, which highly decreased ME1 expression (Figure 4e). ME1 genetic inhibition had no significant impact on cell proliferation in control conditions, whereas ME1 siRNA rescued proliferation in cells treated with cC + C75 as measured by the percentage of bromodeoxyuridine (BrdU)-incorporating cells (Figure 4f). These results suggested that the increase in ME1 activity contributes to the antiproliferative effects of combined AMPK and FASN inhibition on PC cells.

Accumulation of NADPH, NOX activity and oxidative stress in PC cells treated with AMPK and FASN inhibitors

ME1 catalyzes the conversion of malate to pyruvate concomitantly generating NADPH from NADP. Increased ME1 activity (Figure 4d) was fully consistent with the accumulation of NADPH in cells treated with the combination of FASN and AMPK inhibitors (Figure 5a). In cells, NADPH is either used to support FASN-mediated lipid synthesis or is used as a substrate for the NOX, which generates ROS. NOX converts oxygen into superoxide radicals ($O_2^{\bullet -}$), which are then converted into hydrogen peroxide (H_2O_2) by superoxide dismutase. As expected, a significant 2.5-fold increase of NOX activity was measured in cells following treatment with cC + C75 (Figure 5b), which was correlated to a 2.2- and

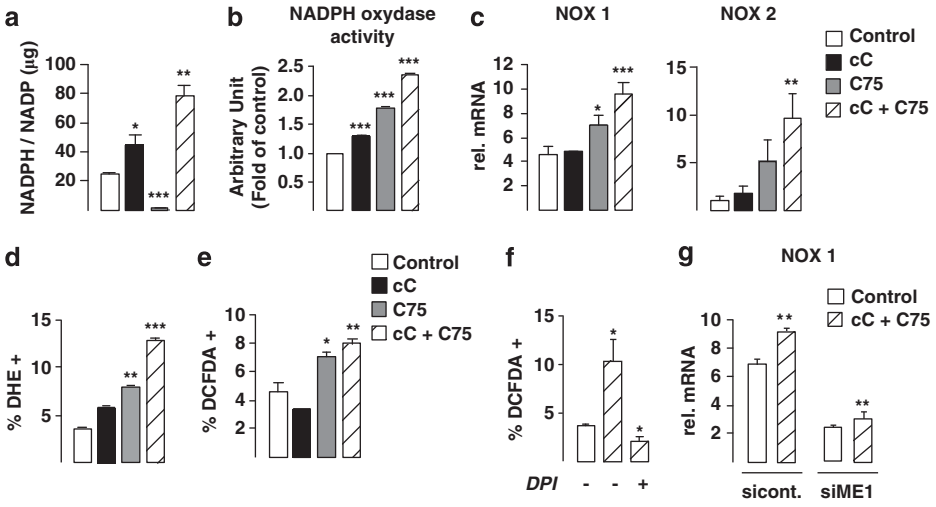

Figure 5. Combined AMPK and FASN inhibition in PC cells is associated with an increased NOX activity and associated ROS production. (**a**) NADPH on NADP cellular ratio was measured in LNCaP cells by colorimetric assay at 48 h following indicated treatments. (**b**) NOX activity was measured by chemiluminescence in the presence of NADPH substrate and lucigenin at 24 h following indicated treatments. (**c**) NOX1 and -2 isoforms mRNA levels were analyzed by RT-qPCR at 24 h following indicated treatments. (**d**, **e**) FACS analysis of cellular ROS production measuring superoxide radicals ($O_2^{\bullet -}$) and H_2O_2 with DHE (**d**) and DCFDA (**e**) fluoroprobes, respectively. (**f**) Co-treatment of cells with 2 μM NOX inhibitor DPI abrogated cC + C75-induced ROS increase, as measured with DCFDA fluoroprobe by FACS analysis. (**g**) Rescue from NOX1 mRNA level induction following cC + C75 treatment was measured by RT-qPCR following LNCaP cell transfection with siRNA against ME1, as compared with control.

9.8-fold induction, respectively, of NOX1 and NOX2 mRNAs (Figure 5c). A subsequent increase in oxidative stress in response to cC + C75 treatment was demonstrated by a threefold increase in the level of superoxide (Figure 5d) and a twofold increase in the level of H_2O_2 (Figure 5e), which was consistent with the increased NOX activity. These results suggested that NOX contributed to ROS generation in PC cells following combined FAS and AMPK inhibition. To test this hypothesis, LNCaP cells were pretreated with diphenyliodonium (DPI), which is a known NOX inhibitor, before cC + C75 treatment. Analysis of ROS production indicated that DPI pre-treatment selectively abrogated the effects of cC + C75 co-treatment on H_2O_2 overproduction, further demonstrating that NOX activity leads to oxidative stress in these cells in response to the combination treatment (Figure 5f). Moreover, genetic inhibition of ME1 in LNCaP cells by siRNA blocked NOX1 mRNA upregulation following cC + C75 co-treatment, strongly suggesting that NADPH production by ME1 activity stimulated NOX activity in PC cells (Figure 5g).

AMPK and FASN inhibition results in the inhibition of cell proliferation and induction of apoptosis in PC cells through NOX-dependent increased oxidative stress

Increased ROS production in response to AMPK and FASN co-inhibition was associated with oxidative stress in PC cells, as demonstrated by the augmentation of lipid peroxidation measured on cellular extracts from LNCaP treated with both cC and C75 (Figure 6a). Oxidative stress was also associated with an upregulation of the expression of antioxidant enzymes such as peroxidase-1, peroxidase-2 or catalase (Figure 6b). To evaluate the implication of ROS overproduction in apoptosis induction following AMPK and FASN inhibitions, LNCaP cells were treated with various antioxidant agents before cC and C75 treatment. Thus, ascorbic acid blocked the induction of ROS generation by cC + C75 treatment in a dose-dependent manner (Figure 6c). ROS production was also significantly reduced by pre-treatment with the antioxidant Trolox (Figure 6c). Interestingly, inhibition of ROS production by antioxidant treatment significantly rescued cell viability (Figure 6d) and abrogated cC + C75-induced apoptosis in LNCaP cells (Figure 6e). Strikingly, inhibition of NOX activity by DPI also abrogated cC + C75-induced apoptosis in these cells (Figure 6f). These results suggested that the oxidative stress, induced by NOX activity, induces apoptosis in cancer cells. Altogether, these results suggested that, in the context of AMPK and FASN co-inhibition, the excess of generated oxidative stress resulting from increased NOX activity leads to apoptosis in PC cancer cells.

DISCUSSION

Cancer cell metabolism is an emerging target for cancer therapeutics. Here we have designed an original experimental therapy that considers metabolic pathways as a very dynamic system that ultimately adapts to specific stress conditions and substrate utilization. On the basis of our results, we propose a new concept in cancer therapy that we call metabolic bioengineering. It is founded in the observation that some specific metabolic pathways are well defined in cancer cells, and that by using inhibitors of specific reactions we can take control of cells' metabolism and direct it toward a particular output of toxic products. Our approach is represented in Figure 7. Cancer cells, in contrast to normal cells, depend on lipid synthesis pathways for survival. Previous studies demonstrated that inhibition of lipid synthesis using FASN inhibitors hampers cancer cell growth and proliferation.[8,9] It was demonstrated that these effects are mediated by the accumulation of malonyl-CoA, which blocks CPT1-mediated FA β-oxidation, leading to the accumulation of ceramide and other proapoptotic lipids (reviewed in Menendez and Lupu[10]). In addition, malonyl-CoA accumulation results in the upregulation of the transcription factor PEA3, which represses the expression of ERBB2, thus abrogating this oncogenic signaling pathway.[11] In this scenario, we designed a combination therapy aiming to force cancer cells to accumulate high levels of malonyl-CoA. We show that co-treatment of cells with FASN and AMPK inhibitors results in additive accumulation of malonyl-CoA in cancer cells. Inhibition of FASN results in decreased malonyl-CoA utilization, whereas inhibition of AMPK ultimately results in the activation of ACC1, and consequently more malonyl-CoA synthesis

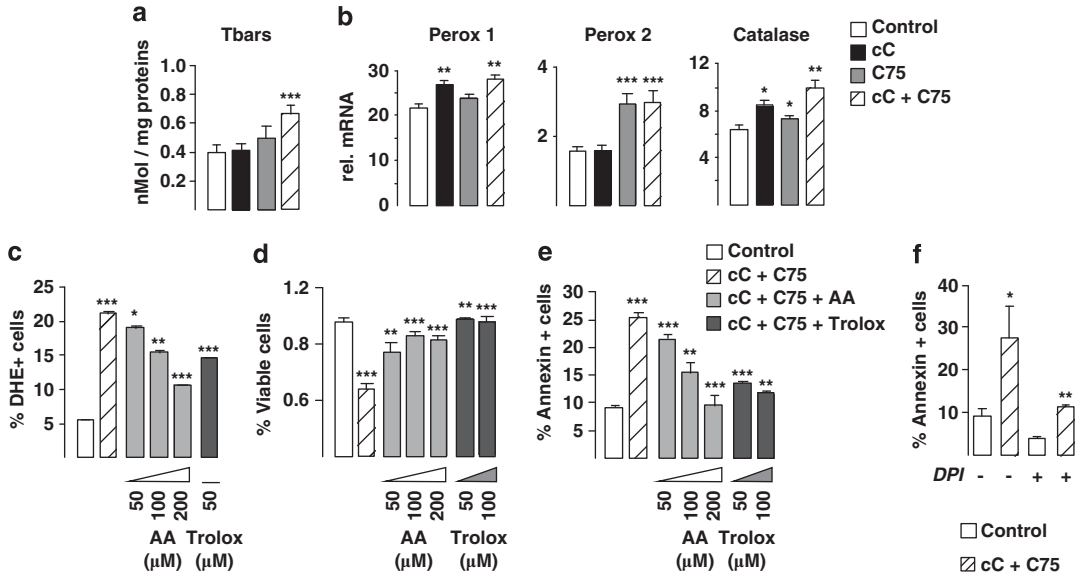

Figure 6. Antiproliferative and proapoptotic effects of AMPK and FASN inhibition in PC cells are mediated by a NOX-dependent ROS overproduction. (**a**) The presence of oxidative stress as a consequence of ROS overproduction following cC + C75 treatment was analyzed by measuring the formation of thiobarbituric acid-reactive substrates (Tbars), indicative of lipid peroxidation, on LNCaP cellular extracts. Values are expressed as mM of malonaldehyde and normalized to protein content. (**b**) The mRNA expression levels of the antioxidant enzymes peroxidase (Perox)-1 and -2 and catalase, as measured by RT-qPCR, were compared following LNCaP treatment, as indicated. (**c**–**e**) Protective effects of antioxidants on ROS production (**c**), cell proliferation (**d**) and apoptosis (**e**) in cC + C75-treated LNCaP cells was conducted by 2-h pre-treatment with increasing amounts of the antioxidants ascorbic acid (AA) and Trolox, as indicated. (**c**) Rescue of ROS overproduction in cC + C75-treated LNCaP cells was assessed by FACS analysis by measuring H_2O_2 content with DHE fluoroprobe following treatment with increasing doses of antioxidants. (**d**) Rescue of cC + C75-treated LNCaP cell proliferation was measured by XTT (2,3-bis-(2-methoxy-4-nitro-5-sulfophenyl)-2*H*-tetrazolium-5-carboxanilide) assay at 48 h following co-treatment with increasing amounts of antioxidants. (**e**) Rescue of cC + C75-treated LNCaP cells from apoptosis induction was measured by FACS analysis of annexin V-FITC + cells at 16 h following co-treatment with increasing amounts of antioxidants. (**f**) Rescue of cC + C75-treated LNCaP cells from apoptosis induction by 6-h co-treatment with 2 μM NOX inhibitor DPI was measured by FACS analysis of annexin V-FITC + cells.

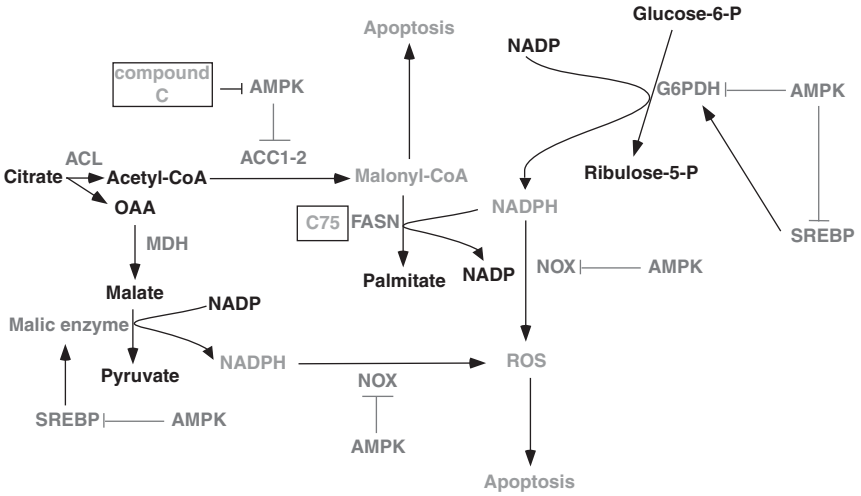

Figure 7. Hypothetical mechanism underlying the proposed metabolic therapy. Inhibition of AMPK, in the context of inactive FASN, influences several metabolic pathways. First, AMPK inhibition activates ACC-mediated malonyl-CoA formation, the accumulation of which has apoptotic effects. Second, AMPK inhibition results in the activation of SREBP and of ME and G6PDH enzymes, resulting in the accumulation of NADPH. Moreover, FASN inhibition leads to further accumulation of NADPH, which is not used as a substrate for *de novo* lipids synthesis. As the NOX enzyme is also activated as a result of AMPK inhibition, excess of NADPH substrate will be converted into ROS. Altogether, this results in an increased apoptosis in cancer cells.

(Figure 7). We showed that accumulation of this lipid precursor results in increased cancer cell death. It is important to stress that the toxic effects of lipid synthesis inhibition are specific of cancer cells, as we showed that *de novo* lipid synthesis pathways are at very low levels in non-cancer prostate cells (Figure 1c and Fritz *et al.*[4]). We also show, however, that inhibition of FASN alone has effects in cell proliferation or apoptosis despite the low accumulation of malonyl-CoA. FASN inactivation is already a potent anti-lipogenic effect. *De novo* FA biosynthesis is required for cancer cells to synthesize new membranes, to generate signaling molecules, such as phosphatidyl inositol, phosphatidyl serine or phosphatidyl choline, which are important factors to

activate proliferative and survival pathways. We can therefore hypothesize that FASN inhibition by itself could lead to these effects independent of malonyl-CoA accumulation.

As our experimental approach is based on the inhibition of AMPK, we further explored the mechanisms underlying the effects of AMPK inhibition in the context of blocked lipid synthesis. AMPK, in addition to blocking ACC1, is also known to inhibit SREBP-1 activity. We showed, consequently, that co-treatment increased the transcriptional activity of SREBP-1, as well as the expression and activity of some of the tested SREBP-1 target genes, in particular *ME* or *G6PDH*. Previous studies using transgenic mice overexpressing SREBP isoforms evidenced a marked increase of mRNAs for NADPH-producing enzymes, such as *ME* or *G6PDH*.[12,13] In the context of concomitant lipid synthesis inhibition, this has several connotations. First, SREBP-1 target gene activation, such as ME or G6PDH, results in the generation of NADPH species in the cell. Under normal conditions, NADPH would be used by FASN as a cofactor for lipid synthesis, whereas under FASN inhibition conditions, such as that used in our study, NADPH would accumulate (Figure 7). AMPK also inhibits NOX enzymes, which convert NADPH into ROS, thus generating oxidative stress. Strikingly, NOX activity was increased secondary to AMPK inhibition in PC cells. We showed that increased NADPH and ME activity was translated into NOX-dependent increase of ROS, which correlated with increased apoptosis in these cells (Figure 7). It is known that ROS generation promotes cancer cell development, but excess ROS is also toxic for cancer cells. Recent studies have shown the therapeutic potential of agents that increase cellular ROS levels to selectively kill cancer cells.[14] Overall, we created in these PC cells a synergistic accumulation of apoptotic signals, that is, malonyl-CoA accumulation and ROS generation, by using the 'metabolic bioengineering' approach. Considering the complexity of metabolic pathways, we strongly believe that many other strategies using similar approaches will emerge in the near future.

We show here that AMPK inhibition results in proliferation arrest and apoptosis of cancer cells, whereas AMPK activation is regarded as an emerging therapy for cancer treatment.[15] To explain this apparent paradox, we have to consider the effects of AMPK in the proper context. AMPK activators are mimicking energy deprivation in cancer cells, thus inhibiting biosynthetic processes, including cell proliferation. Moreover, under energetic stress conditions, such as that observed in cancer cells, AMPK activation can have a protective effect against apoptosis and facilitate cancer cell survival.[16] In addition, AMPK activation could be required for the observed metabolic switch in cancer cells (reviewed in Viollet *et al.*[17]). Finally, AMPK may protect cancer cells from oxidative stress.[18] When lipid synthesis pathways are inhibited, the antiproliferative effects of AMPK activation are, however, lost. Furthermore, in this scenario, inhibition of AMPK forces the system toward the generation of oxidative stress, ultimately resulting in cancer cell death, as we have demonstrated.

In conclusion, a better knowledge of metabolic pathways in cancer cells will facilitate the design of targeted therapies that we prove promising for the treatment of cancer.

MATERIALS AND METHODS

Cell culture, transient transfections and RNA interference experiments

The benign PNT2 prostate epithelial cell line was obtained from the European Collection of Cell Cultures (Sigma Aldrich, Saint Quentin Fallavier, France). The androgen-sensitive LNCaP and the androgen-independent C4-2 human prostate carcinoma cell lines were purchased from Viromed Laboratory Inc. (Minnetonka, MN, USA). The metastatic androgen-independent PC-3 prostate carcinoma cell lines were kindly provided by Dr Patrick Balaguer (IRCM, Montpellier, France). Monolayer cell cultures were maintained in RPMI 1640 medium (Invitrogen, Cergy, France) supplemented with 10% fetal calf serum, 100 U/ml penicillin, 100 μg/ml streptomycin, 10 mM HEPES and 1.0 mM sodium pyruvate (Invitrogen) at 37 °C in 5% CO_2. The transcriptional activity of SREBP-1 was analyzed by performing transient co-transfections with 0.25 μg SREBP-1 or control vector and 0.25 μg FASN promoter luciferase (Luc) reporter or control vector. The transcriptional activity of ME1 was analyzed by performing transient transfections with 0.25 μg ME1 promoter Luc reporter (LightSwitch Luciferase) or control Luc vector (SwitchGear Genomics, Menlo Park, CA, USA), according to the manufacturer's instructions. Renilla luciferase activities in cell lysates were normalized relative to the β-galactosidase activity to correct for differences in transfection efficiency. For siRNA experiments, transfection of LNCaP or C4-2 cells was carried out with predesigned ON-TARGET plus smart pool siRNA oligonucleotide control or by targeting the human AMPKα1/2 (IDT, Paris, France) or the human ME1 sequence (Dharmacon, Lafayette, CO, USA). Nucleofaction of cells with 2.5 μg of siRNA was performed on 2×10^6 cells using the Amaxa nucleofactor R kit (Lonza, Cologne, Germany). At 24 and 48 h after transfection, cells were processed for cell proliferation by cell counting or BrdU staining and harvested for annexin staining or RNA analysis.

Animal experiments

Male athymic nude mice (Foxn1nu/nu) (Harlan, Grannat, France) were used at the age of 6–7 weeks (weight 25–30 g). All procedures were performed in compliance with the European Convention for the Protection of Vertebrate Animals Used for Experimentation (animal house agreement no. B-34-172-27, authorization for animal experimentation no. 34.324). Animals were killed before they became compromised. Xenografts were established by subcutaneously injecting 2×10^6 LNCaP, C4-2 cells or PC-3 in 100 μl of Matrigel solution. For curative experiments, tumors were allowed to grow until they were measurable with a caliper. In each group, the mice were randomized according to their established tumor volume and given either the AMPK inhibitor cC at 10 mg/kg, the FASN inhibitor C75 at 10 mg/kg or both cC and C75 inhibitors (Sigma Aldrich) at 10 mg/kg, in 100 μl of a Labrafil-DMA-Tween-80 solution (89:10:1) (treated group) or vehicle alone (control group), by daily intraperitoneal injections 5 days a week. Tumor volume measurements were taken two to three times a week and calculated according to the following formula: length × width × height × 0.5236. Data are expressed as the mean tumor volume ± s.e.m. Experiments were carried out at least two times for each tested condition. Mice were bled at the retro-orbital sinus for hematocrit analysis. At the time of killing, tumors were excised and either fixed in 4% formalin for immunohistological analysis or prepared for FA analysis.

Quantitative real-time PCR

For gene expression analysis following treatment of cells with different inhibitors, RNA isolation, reverse transcription (RT) and quantitative (q) real-time polymerase chain reaction (PCR) were carried out as described previously.[4] qPCR was conducted on the ABI Prism 7300 Sequence detection System software (Applied Biosystems, Life Technologies SAS, Villebon sur Yvette, France), using the SYBR Green Light Cycler Master Mix (Eurofins MWG Operon, Roissy CDG, Italy) and the oligonucleotides specific for human G6PDH, ATP-citrate lyase, ME1, malate dehydrogenase-1 and -2, NOX1 and -2, peroxidase-1 and -2 isoforms and catalase. Values are expressed as the relative mRNA level of specific target gene normalized to 18S levels, as obtained using the formula $2^{-(\Delta Ct)}$.

Malonyl-CoA measurement

Quantification of malonyl-CoA concentration in whole-cell lysates from PNT2, LNCaP and C4-2 cells was realized by enzyme-linked immunosorbent assay using the commercial kit according to the manufacturer's instructions (antibodies online.com). Briefly, subconfluent cell cultures grown in 6-well plates were treated for 24 h with cC and/or C75 inhibitors, and whole-cell lysates were subjected to several freeze–thaw cycles and then centrifuged. Malonyl-CoA in the supernatant was detected by specific biotin-conjugated antibody on pre-coated 96-well plates and revealed with avidin-conjugated horseradish peroxidase. Values are expressed as nM malonyl-CoA and were normalized to total protein content (mean ± s.e.m.).

Acetyl-CoA measurement

Concentration of acetyl-CoA in whole-cell lysates from PNT2, LNCaP and C4-2 cells was measured by fluorescence assay using a commercial kit according to the manufacturer's instructions (Abcam). Values are

expressed as μM malonyl-CoA and were normalized to total protein content (mean ± s.e.m.).

Measurement of *de novo* FA synthesis

Subconfluent cultures of PNT2, LNCaP, C4-2 or PC-3 cells grown in 6-well plates were treated overnight with cC and/or C75 inhibitors in serum and FA-free Dulbecco's modified Eagle's medium supplemented with 0.2% bovine serum albumin. Cultures were then labeled in triplicate with 1.0 μCi of [^{14}C]acetate for 6 h. Total lipids were extracted two times with 5 ml of Folch mixture (chloroform:methanol, 2:1 (v/v)) and 500 μl of water,[19] and then dried under gaseous nitrogen. Labeled lipids were then subjected to TLC in hexane:diethyl ether:acetic acid 90:10:1 (v/v) to separate cholesterol ester, triglycerides and phospholipids. Air-dried plates were scanned on a PhosphorImager, and FA spots on TLC were analyzed with the Typhoon 9200 PhosphorImager software (Amersham Biosciences, GE Healthcare Europe, Velizy-Villacoublay, France). Values were normalized to protein contents and areas are expressed as mean ± s.e.m.

FA analysis

Total lipids from C4-2 tumors xenografts were extracted three times with folch mixture, converted to fatty methyl esters as described previously[4] and subjected to gas chromatography identification. Gas chromatography was conducted with a Thermo GC fitted with a flame ionization detector. A supelcowax-10 fused silica capillary column (60 m × 0.32 mm i.d., 0.25 μM film thickness) was used, and the oven temperature was programmed from 50 to 200 °C, increased 20 °C/minute, held for 50 min, increased 10 °C/min to 220 °C and held for 30 min. Values were normalized to tissue weight and are expressed as mean ± sem.

Proliferation assay

Proliferation of LNCaP or C4-2 cells at 24, 48 and 72 h following the addition of inhibitors in dimethyl sulfoxide or dimethyl sulfoxide alone at the indicated doses was determined by cell counting using an hematocytometer, as described previously.[4]

XTT proliferation assay

LNCaP or C4-2 cells were seeded in triplicate 96-well dishes containing 10^4 cells per well. At 48 h after treatment with inhibitors in dimethyl sulfoxide or dimethyl sulfoxide alone, the enzymatic reduction of tetrazolium salt XTT (2,3-bis-(2-methoxy-4-nitro-5-sulfophenyl)-2*H*-tetrazolium-5-carboxanilide; Roche Applied Science, Meylan, France) to formazan was quantified by optical density reading at 490 nm in each well, and normalized with a reference wavelength at 650 nm in a microplate reader.

BrdU staining

The percentage of proliferative BrdU-incorporating LNCaP and C4-2 cells was measured as described previously.[4]

Fluorescence-activated cell sorting analysis of apoptosis and ROS production

Induction of apoptosis in subconfluent LNCaP or C4-2 cells following 16 h treatment with either 1 μg/ml cC, 7 μg/ml C75 or both cC + C75 inhibitors was determined by fluorescence-activated cell sorting (FACS) analysis by measuring the percentage of FITC-conjugated annexin V+ cells as described previously.[4] Caspase inhibition was achieved by adding 20 μmol/l of caspase inhibitor qVD-oph (MP Biomedicals SARL, Illkirch, France) 30 min before the apoptotic stimuli. Induction of ROS in subconfluent LNCaP or C4-2 cells following a 6-h treatment with either 1 μg/ml cC, 7 μg/ml C75 or both cC + C75 inhibitors was determined by FACS analysis by measuring he production of cellular superoxide ($O_2^{\bullet -}$) and H_2O_2 using the fluoroprobes dihydroethidium (DHE) at 2 μM and carboxy-H_2DCFDA (DCFDA) at 10 μM, respectively. To analyze the effects of antioxidants on apoptosis and ROS production, cells were pre-treated for 2 h with increasing doses of ascorbic acid (from 50 to 200 μM) or Trolox (from 50 to 100 μM) and then incubated with cC, C75 or both cC + C75 in the presence of antioxidants. To analyze the effects of NOX inhibition on apoptosis induction and on ROS production, LNCaP or C4-2 cells were pre-treated for 2 h with NOX inhibitor DPI at 2 μM and then incubated for an additional 4 h with either cC 1 μg/ml, C75 7 μg/ml or both cC + C75 in the presence of DPI. FACS experiments were performed using a Becton Dickinson FACScalibur with 488-nm laser excitation, and analyzed with the CellQuest Pro software. Data are expressed as the mean percentage of positive cells for the indicated fluorescence intensity.

Immunohistochemistry (IHC)

Immunohistochemical analyses of Ki67 and cleaved caspase-3 expression were performed on 5 μM paraffin-embedded sections of C4-2 tumor xenografts. Briefly, after antigen retrieval, deparaffinized sections were blocked for Fc receptors with PBS containing 5% goat serum and then incubated with the corresponding anti-Ki67 rabbit antibody (1:500; Abcam, Strasbourg, France) or cleaved caspase-3 rabbit antibody (1:500; Cell Signaling, Saint Quentin Yvelines, France) in PBS-Tween 0.1%, overnight at 4 °C. Staining was revealed with a peroxidase-conjugated anti-rabbit secondary antibody (1:100; Jackson Immunoresearch, Interchim, Montlucon, France) and with the DAB chromogen (DAKO, Glostrup, Denmark) as substrate. Sections were counterstained with Mayer's hematoxylin.

Immunocytochemistry

Immunocytochemical analysis of cleaved caspase-3 and cytochrome C expressions were performed on PNT2, LNCaP, and C4-2 cells grown on coverslip. Briefly, after fixation in 4% PFA and permeabilization with 0.5% Triton X-100, cells were incubated with blocking buffer (PBS- 1% BSA). Cleaved caspase-3 expression staining was detected with an cleaved caspase-3 (Asp175) rabbit primary antibody, 1:500 (Cell signaling) for 2 hour at 37 °C and revealed with a Alexa Fluor 488nm-labeled goat anti-rabbit secondary antibody (Jackson Immunoresearch), 1:500 for 45 min at 37 °C. Then cytochrome C expression staining was detected with an cytochrome C mouse primary antibody, 1:40 (BD Pharmingen) overnight at 4 °C and revealed with a Alexa Fluor 594 nm-conjugated goat anti-mouse secondary antibody (Jackson Immunoresearch), 1:500 for 45 min at 37 °C. In the last wash, cells were labeled with with dapi for 5 min at room temperature. Slides were mounted in mowiol and analyzed rapidly.

Lipid peroxidation

Lipid peroxidation was determined by measuring the formation of thiobarbituric acid-reactive substrates in LNCaP cellular extracts. Concentrations were measured against a standard curve obtained with malonaldehyde. Thiobarbituric acid-reactive substrate values were expressed as mM malonaldehyde/mg protein.

Protein extracts and immunoblot analysis

Protein extracts and sodium dodecyl sulfate–polyacrylamide gel electrophoresis, electrotransfer and immunoblotting were carried out as described previously.[20] The primary antibodies rabbit anti-AMPK, rabbit anti-phospho-AMPK (Thr172), rabbit anti-phospho-ACC (Ser79) and rabbit anti-cleaved caspase-3 were purchased from Cell Signaling Technology (Ozyme, Saint Quentin Yvelines, France). The primary antibody rabbit anti-ME1 was purchased from Abcam. The primary antibody mouse anti-tubulin-α was purchased from Lab Vision (Thermo Fisher Scientific, Microm France, Francheville, France).

Determination of ME activity

ME activity was determined as described previously,[21] with some modifications, by measuring the fluorescence associated with the generation of β-NADPH during conversion of L-malate to pyruvate in the presence of β-NADP, according to the reaction: L-malate + β-NADP → pyruvate + CO_2 + β-NADPH. Briefly, protein extracts (50 μg) were added to a 100 mM Tris buffer (pH 7.4) containing 20 mM $MnCl_2$, 20 mM NADP+ and 100 mM malate, in a cuvette positioned inside a temperature-controlled chamber maintained at 25 °C. Fluorescence was measured with a 340-nm excitation and 460-nm emission on a fluorescence spectrophotometer. Values are expressed as ABS/min/mg proteins.

Determination of NADPH cellular content

NADP and NADPH concentrations were determined on fresh LNCaP or C4-2 cellular extracts by colorimetric assay using the EnzyChrom TM NADP+/NADPH Assay Kit (Gentaur, Paris, France), as described by the manufacturer.

Determination of NOX activity

NOX activity was measured in whole LNCaP or C4-2 cells by using lucigenin-derived chemiluminescence as described previously, with some

modifications.[22] Briefly, 5×10^5 cells were diluted in 200 µl of 50 mM potassium phosphate buffer (pH 7.0) containing protease inhibitor cocktail and 1 mM ethylene glycol tetraacetic acid. A volume of 180 µl of the reaction mixture containing 1 mM ethylene glycol tetraacetic acid, 150 mM sucrose, 100 µM NADPH and 5 µM lucigenin was immediately added to 20 µl of the cell suspension in a dark-adapted 96-well plate, and chemiluminescence was measured at 8-s intervals for 20 min. Data are expressed as mean relative luciferase units.

Statistical analysis

Results are expressed as mean ± s.e.m. of triplicates. Figures show representative results of at least two independently performed experiments. Statistical analyses were performed with unpaired Student's *t*-test. Differences were considered statistically significant at $P<0.05$ ($^*P<0.05$, $^{**}P<0.01$ and $^{***}P<0.001$).

CONFLICT OF INTEREST

The authors declare no conflict of interest.

ACKNOWLEDGEMENTS

Members of Fajas' lab are acknowledged for support and discussions. This work was supported by grants from Ligue Contre le Cancer, Agence Nationale de la Recherche (ANR) and Institut National du Cancer (INCA).

Author contributions: JPC and LF designed the study; VF planned the experiments; VF, CH, ZB, SH, MC, FM and FC performed the experiments; and VF and LF wrote the manuscript.

REFERENCES

1 Kuhajda FP. Fatty-acid synthase and human cancer: new perspectives on its role in tumor biology. *Nutrition* 2000; **16**: 202–208.
2 Brusselmans K, Vrolix R, Verhoeven G, Swinnen JV. Induction of cancer cell apoptosis by flavonoids is associated with their ability to inhibit fatty acid synthase activity. *J Biol Chem* 2005; **280**: 5636–5645.
3 Brusselmans K, De Schrijver E, Verhoeven G, Swinnen JV. RNA interference-mediated silencing of the acetyl-CoA-carboxylase-alpha gene induces growth inhibition and apoptosis of prostate cancer cells. *Cancer Res* 2005; **65**: 6719–6725.
4 Fritz V, Benfodda Z, Rodier G, Henriquet C, Iborra F, Avances C *et al.* Abrogation of *de novo* lipogenesis by stearoyl-CoA desaturase 1 inhibition interferes with oncogenic signaling and blocks prostate cancer progression in mice. *Mol Cancer Ther* 2010; **9**: 1740–1754.
5 Fritz V, Fajas L. Metabolism and proliferation share common regulatory pathways in cancer cells. *Oncogene* 2010; **29**: 4369–4377.
6 Pizer ES, Thupari J, Han WF, Pinn ML, Chrest FJ, Frehywot GL *et al.* Malonyl-coenzyme-A is a potential mediator of cytotoxicity induced by fatty-acid synthase inhibition in human breast cancer cells and xenografts. *Cancer Res* 2000; **60**: 213–218.
7 Thupari JN, Pinn ML, Kuhajda FP. Fatty acid synthase inhibition in human breast cancer cells leads to malonyl-CoA-induced inhibition of fatty acid oxidation and cytotoxicity. *Biochem Biophys Res Commun* 2001; **285**: 217–223.
8 Kuhajda FP, Jenner K, Wood FD, Hennigar RA, Jacobs LB, Dick JD *et al.* Fatty acid synthesis: a potential selective target for antineoplastic therapy. *Proc Natl Acad Sci USA* 1994; **91**: 6379–6383.
9 Swinnen JV, Brusselmans K, Verhoeven G. Increased lipogenesis in cancer cells: new players, novel targets. *Curr Opin Clin Nutr Metab Care* 2006; **9**: 358–365.
10 Menendez JA, Lupu R. Fatty acid synthase and the lipogenic phenotype in cancer pathogenesis. *Nat Rev Cancer* 2007; **7**: 763–777.
11 Menendez JA, Ropero S, Mehmi I, Atlas E, Colomer R, Lupu R. Overexpression and hyperactivity of breast cancer-associated fatty acid synthase (oncogenic antigen-519) is insensitive to normal arachidonic fatty acid-induced suppression in lipogenic tissues but it is selectively inhibited by tumoricidal alpha-linolenic and gamma-linolenic fatty acids: a novel mechanism by which dietary fat can alter mammary tumorigenesis. *Int J Oncol* 2004; **24**: 1369–1383.
12 Korczynska J, Stelmanska E, Nogalska A, Szolkiewicz M, Goyke E, Swierczynski J *et al.* Upregulation of lipogenic enzymes genes expression in white adipose tissue of rats with chronic renal failure is associated with higher level of sterol regulatory element binding protein-1. *Metabolism* 2004; **53**: 1060–1065.
13 Stelmanska E, Korczynska J, Swierczynski J. Tissue-specific effect of refeeding after short- and long-term caloric restriction on malic enzyme gene expression in rat tissues. *Acta Biochim Pol* 2004; **51**: 805–814.
14 Huang P, Feng L, EA Oldham, MJ Keating, W Plunkett. Superoxide dismutase as a target for the selective killing of cancer cells. *Nature* 2000; **407**: 390–395.
15 Fogarty S, Hardie DG. Development of protein kinase activators: AMPK as a target in metabolic disorders and cancer. *Biochim Biophys Acta* 2010; **1804**: 581–591.
16 Kato K, Ogura T, Kishimoto A, Minegishi Y, Nakajima N, Miyazaki M *et al.* Critical roles of AMP-activated protein kinase in constitutive tolerance of cancer cells to nutrient deprivation and tumor formation. *Oncogene* 2002; **21**: 6082–6090.
17 Viollet B, Horman S, Leclerc J, Lantier L, Foretz M, Billaud M *et al.* AMPK inhibition in health and disease. *Crit Rev Biochem Mol Biol* 2010; **45**: 276–295.
18 Zhang J, Bowden GT. UVB irradiation regulates Cox-2 mRNA stability through AMPK and HuR in human keratinocytes. *Mol Carcinogen* 2008; **47**: 974–983.
19 Folch J, Lees M, Sloane Stanley GH. A simple method for the isolation and purification of total lipides from animal tissues. *J Biol Chem* 1957; **226**: 497–509.
20 Sarruf DA, Iankova I, Abella A, Assou S, Miard S, Fajas L. Cyclin D3 promotes adipogenesis through activation of peroxisome proliferator-activated receptor gamma. *Mol Cell Biol* 2005; **25**: 9985–9995.
21 Geer BW, Krochko D, Williamson JH. Ontogeny, cell distribution, and the physiological role of NADP-malic enxyme in Drosophila melanogaster. *Biochem Genet* 1979; **17**: 867–879.
22 Eid AA, Ford BM, Block K, Kasinath BS, Gorin Y, Ghosh-Choudhury G *et al.* AMP-activated protein kinase (AMPK) negatively regulates Nox4-dependent activation of p53 and epithelial cell apoptosis in diabetes. *J Biol Chem* 2010; **285**: 37503–37512.

Supplementary Information accompanies the paper on the Oncogene website (http://www.nature.com/onc)